Energy flux measurements in high power impulse magnetron sputtering

Daniel Lundin, Marc Stahl, Holger Kersten and Ulf Helmersson

Original Publication:

Daniel Lundin, Marc Stahl, Holger Kersten and Ulf Helmersson, Energy flux measurements in high power impulse magnetron sputtering, 2009, JOURNAL OF PHYSICS D-APPLIED PHYSICS, (42), 18, 185202.
http://dx.doi.org/10.1088/0022-3727/42/18/185202

Thermal flux measurements in high power impulse magnetron sputtering

Daniel Lundin[1], Marc Stahl[2], Holger Kersten[2] and Ulf Helmersson[1]

[1] *Plasma & Coatings Physics Division, IFM-Materials Physics, Linköping University, SE-581 83 Linköping, Sweden*

[2] *University of Kiel, Institute of Experimental and Applied Physics, Leibnizstrasse 11-19, 24098 Kiel, Germany*

E-mail: danlu@ifm.liu.se

Abstract

The total energy flux in a high power impulse magnetron sputtering (HiPIMS) plasma has been measured using thermal probes. Radial flux (parallel to the magnetron surface) as well as axial flux (perpendicular to the magnetron surface) were measured at different positions, and resulting energy flux profiles for the region between the magnetron and the substrate are presented. It was found that the substrate heating is reduced in the HiPIMS process compared to conventional direct current magnetron sputtering (DCMS) at the same average power. On the other hand, the energy flux per deposited particle is higher for HiPIMS compared to DCMS, when taking into account the lower deposition rate for pulsed sputtering. This is most likely due to the highly energetic species present in the HiPIMS plasma. Furthermore, the heating due to radial energy flux reached as much as 60 % of the axial energy flux, which is likely a result of the anomalous transport of charged species present in the HiPIMS discharge. Finally, the experimental results were compared to theoretical calculations on energy flux of charged species, and they were found to be in good agreement.

1. Introduction

Plasma-wall interactions are very important in a large variety of plasma applications e.g. etching, deposition of thin films, and surface modification. The thermal and energetic conditions at the substrate surface influenced by the different plasma species such as electrons, ions, and neutrals determine the elementary processes (adsorption, diffusion, chemical reactions) as well as the microstructure and stoichiometry of film growth [1, 2]. The effect of energy per incoming particle and the particle flux is therefore essential in plasma processing of solid surfaces, particularly in the case of thin film growth [3, 4, 5, 6]. The product of these two quantities constitutes the energy flux, which is a key parameter when investigating the energetic conditions at the surface of the growing film.

High power impulse magnetron sputtering (HiPIMS) is one of the most promising techniques for improving common magnetron sputtering used in many industrial processes for thin film deposition [7]. The HiPIMS plasma generates large quantities of highly energetic ions [8] with, in some cases, a directed flux of charged species [9]. The transport of these energetic particles is not fully understood, but it is clear that they have a dramatic effect on thin film growth, such as densification and improved adhesion [6, 10].

In this study the total energy flux in a high power impulse magnetron sputtering (HiPIMS) plasma has been investigated using thermal probes. The average power was varied and the results were compared to conventional direct current magnetron sputtering (DCMS) discharges. Furthermore, the influence of bias voltage on the thermal probe was investigated in order to gain insight into the contributions of the different charge carriers. The work also include thermal probe studies of directionality of the energetic fluxes from both ions and electrons present in the plasma. From the deposited power (i.e. energy flux) the temperature evolution at different positions during HiPIMS operation can be estimated. This is important when coating thermally sensitive substrates such as plastics, but also for a general understanding of the HiPIMS-plasma by fitting to modeling results [11].

2. Experimental details

A standard planar circular magnetron with a diameter of 15 cm, equipped with a Ti (99.9 %) target mounted in a cylindrical vacuum chamber (height 70 cm, diameter 44 cm) was used in the present experiments. The chamber was pumped by a turbo-molecular pump to a pressure of about 1.5×10^{-4} Pa, after which 0.53 Pa of an inert gas (Ar with a minimum purity of 99.9997 %) was let into the chamber. High-voltage pulses were applied between the cathode (target) and the chamber walls using a HiPIMS power supply (Sinex 3, Chemfilt Ionsputtering

AB). In this work 100 µs pulses were used at a repetition frequency of 100 Hz. The applied voltage was varied between 720 – 800 V resulting in a peak current of about 270 - 500 A and an average power of approximately 500 - 615 W. For DCMS reference measurements the same power supply was used to deliver constant voltage (~ 330 V) and current (~ 1.5 A) to match the average power in the HiPIMS discharge.

The energy flux from the plasma was measured using several identical compact thermal probes. A sketch of the probe is shown in Figure 1. The probe was mounted on a movable metal rod for scans taken at different axial as well as radial positions as seen in Figure 2. Furthermore, the probe and rod could be rotated in order to measure directional fluxes. The thermal probe consisted of a ceramic shield (Marcor^{TM}) onto which a thermocouple (type K) was brazed. The probe (substrate) was connected only to the thermocouple and a wire for applying an external bias. In all experiments a copper plate with a diameter of 20 mm and a thickness of 0.1 mm was used as a substrate dummy. The measured signal (40.44 µV/°C) was amplified with cold junction compensation and an ice point reference coupled to an amplifier and a low-pass filter with a cutoff frequency of 340 Hz, and recorded in 10 Hz using a 13-bit multi I/O card. The data was analyzed using a program developed in LabVIEW^{TM}.

The principle for measuring the energy flux is based on the rate of change in temperature of the substrate, $\frac{dT_S}{dt}$, which implies measuring the temperature characteristic during the heating process during plasma-on, and the cooling after the plasma has been switched off (Figure 3) [12]. The change of enthalpy of the substrate can be described by

$$\dot{H} = C_S \frac{dT_S}{dt}, \tag{1}$$

where C_S is the absolute heat capacity of the substrate (probe) including the connected wires. The power balance during the heating process can be described by

$$\dot{H}_{heat} = P_{in} - P_{out}, \tag{2}$$

and during the cooling process by

$$\dot{H}_{cool} = -P_{out} \,. \tag{3}$$

If the incoming power, P_{in}, is constant during the heating process and the heat loss, P_{out}, is only a function of T_S, then for each temperature, $\tilde{T}$, measured during the heating and the following cooling processes the incoming power can be calculated by subtracting eq. (3) from eq. (2) such that

$$P_{in}\left(\tilde{T}\right) = \left[\dot{H}_{heat} - \dot{H}_{cool}\right]_{\tilde{T}} = C_S \left[\left(\frac{dT_S}{dt}\right)_{heat} - \left(\frac{dT_S}{dt}\right)_{cool}\right]_{\tilde{T}} . \tag{4}$$

If the slopes of $\frac{dT_S}{dt}$ are determined under the condition that the measurement starts and ends at equilibrium temperature together with the exact knowledge of the heat capacity, then P_{in} can easily be determined. For error estimations the standard deviation is also obtained from solving eq. (4). By dividing P_{in} by the probe surface area the total energy flux, J_{tot}, is obtained.

The heat capacity, C_S, is measured by applying a known power to the substrate surface e.g. by using a laser [13]. In the present work C_S was in this way estimated to an average of 0.3 J/K for all probes used. Note that a much higher accuracy was achieved for the individual cases. The error of the calibration was added to the error of $P_{in}\left(\tilde{T}\right)$ to obtain a total error of the energy flux measurements of about 5 %.

The energy flux consists of different contributions, such as radiation from the environment (plasma and chamber walls) as well as kinetic and potential energy from energetic particles in the flux. These different constituents are not easily separated in any measurement, but by a combination of several experiments it is possible to map out the energy transfer in more detail. The contribution of secondary electrons must be taken into account as the probe is moved closer to the cathode while facing the cathode surface. The general expression for the energy flux given as power per area can be summarized as

$$J_{tot} = J_i + J_e + J_{rec} + J_n + J_{ch} + J_{rad} \tag{5}$$

where J_i is energy flux by ions and J_e is the electron energy flux including secondary electrons. Other contributing terms are the energy release due to recombination of electrons and ions, J_{rec}, energy flux by neutrals, J_n, energy flux by chemical reactions on the surface, J_{ch}, and energy flux by radiation towards the surface, J_{rad}. In this work J_{ch} can be neglected, since there are no exothermic reactions between Ar, Cu and Ti. The other terms will be further developed in section 3.3 concerning a model fit of results obtained by biasing the thermal probe.

3. Results and discussion

3.1. Spatially resolved measurements

The radial (ρ) as well as axial (z) distribution of the energy flux in a HiPIMS plasma of approximately 500 W average power is presented in Figure 4. The thermal probe is facing the magnetron, and is thus picking up the same axial heat flux as a substrate would for the same position. The shape of the energy flux profile indicates that the total heat flux increases towards the surface of the magnetron, and peaks in a region between the race track (ρ ~ 4.5 cm) and the rim of the magnetron. Directly in front of the cathode (z ~ 4 cm) the energy flux is twice as large at ρ ~ 8 cm compared to the center at ρ ~ 0 cm. As we move away from the cathode surface the energy flux gets more homogeneously distributed, and at z > 10 cm the radial variation of the energy flux is rather small. Outside the magnetron (ρ > 8 cm) the flux decreases rapidly (not shown in the figure).

A comparison of the energy flux between HiPIMS and DCMS at approximately the same average power is presented in Figure 5 for different axial positions. The probe was placed above the race track of the circular magnetron ($\rho = 4.5\,\text{cm}$) facing the magnetron surface. In all cases the measured values for HiPIMS are lower than those of the DCMS discharge. The fraction J_{HiPIMS}/J_{DCMS} can be estimated to 32-48 % depending on the axial distance. Previous measurements using the same setup [9] show that the deposition rate ratio for Ti between DCMS and HiPIMS is about $rate_{HiPIMS}/rate_{DCMS} = 0.2$. Taking this into account one can conclude that 90 % more energy per particle is deposited on the substrate in the HiPIMS case. This is not surprising when considering that there is a much larger proportion of highly energetic ions in the HiPIMS discharge [8].

Furthermore, the same data was used to estimate the fraction of the total applied discharge power used for substrate heating in HiPIMS and DCMS. A discharge power of about 500 W results in a power density of 2.83 W/cm^2 on the target (15 cm in diameter). From Figure 5 the position $z = 10\,\mathrm{cm}, \rho = 4.5\,\mathrm{cm}$ was chosen, since it is a commonly used target-to-substrate distance for this deposition system and located at the same radial position as the race track. For the HiPIMS case the average energy flux is about 120 mW/cm^2, resulting in 4 % of the average discharge power is converted into heating the substrate. The corresponding value for the DCMS case is 300 mW/cm^2, i.e. about 10 % of the discharge power is converted into substrate heating. These values are in line with previous work on radio frequency (RF) plasmas by Wolter *et al*. where they conclude that about 7 % of the discharge power in an RF discharge is taken up at the substrate position [13]. It should be noted that the exact values are hard to establish, since they vary depending on the substrate location. For the HiPIMS case a value of more than 10 % is reached at a few centimeters from the target. At these small distances the energetic bombardment is rather high, which may induce compressive stress as the bombarding species are distorting the lattice of the sputtered films (so called atomic-peening mechanism) [14]. If adhesion is not sufficient the stress can promote peeling and films grown at this position are likely to flake off the substrate.

The energy flux measurements can also give an estimate of the maximum temperature reached during deposition for both these techniques. The maximum (equilibrium) temperature for HiPIMS was approximately 70 ºC and about 140 ºC for DCMS, using the same probe position as was done before ($z = 10\,\mathrm{cm}, \rho = 4.5\,\mathrm{cm}$). These values are below the limit for many thermally sensitive substrates, such as Kapton® E (DuPont™), used as a dielectric substrate for circuits and interconnects, which is thermally stable below 150 ºC [15].

3.2. Perpendicular energy flux

Previous investigations on energy flux have focused on the axial flux [13, 16], since thin film deposition is often performed by letting the substrate surface face the cathode. Recent publications on plasma transport in HiPIMS discharges have shown that the cross-**B** conductivity, which governs the transport of charged species across magnetic field lines, is about an order of magnitude higher at peak current for HiPIMS [17, 18] compared to DCMS [19, 20]. This so-called anomalous transport is involved both in the ion motion [9] and probably also in anomalous heating, which causes a high energy tail in the electron energy distribution. By looking at the forces involved in the charged particle transport it has been found that the azimuthally rotating electrons (of which one part constitutes the Hall current) exert a volume force on the ions tangentially outwards from the circular race track region [9]. The effect of having an anomalous transport would therefore be a large fraction of highly energetic ions being transported sideways and lost to the walls. It is thus necessary to investigate to what extent this energetic flux, which is directed radially outwards from the magnetron, contributes to heating the substrate.

The radial flux component has been measured (Figure 6), where the energy flux is perpendicular to the magnetron surface. The measurements were performed at different axial positions and for two different powers. The probe was placed outside the rim of the magnetron at ρ = 15 cm. It can clearly be observed that there is a substantial heating originating from this type of flux with a peak in the energy flux around z ~ 10 cm. For z < 4 cm it is likely that the probe is partly shadowed by the ground shield of the magnetron, and thus resulting in a sharp decrease in the measurements.

In order to estimate the importance of this type of flux the fraction between the radial flux, J_ρ, (parallel to the cathode surface) versus the axial flux, J_z, (perpendicular to the cathode surface) was measured. In this work three different positions have been chosen based on data in Figure 4 and from additional measurements on J_ρ: (1) At the centre of the magnetron (2) above the target race track, and (3) at the rim of the magnetron. The results are summarized in Table 1.

Table 1. A comparison between radial and axial energy flux in a HiPIMS discharge.

Position	Radial flux, J_ρ [mW/cm^2]	Axial flux, J_z [mW/cm^2]
$z = 7$ cm, $\rho = 0$ cm	37	141
$z = 7$ cm, $\rho = 4.5$ cm	83	182
$z = 7$ cm, $\rho = 7$ cm	163	280

From Table 1 we conclude that even for the center position ($z = 7$ cm, $\rho = 0$ cm), where the cross-field transport is expected to be the weakest, the magnitude of the radial flux is still more than 25 % of the axial flux. When moving radially outwards J_ρ increases and peaks at the outer edge of the cathode ($z = 7$ cm, $\rho = 7$ cm) where J_ρ is about 60 % of J_z. For $\rho > 7$ cm the radial energy flux decreases again (not shown here). Moreover, from profiles of the deposition rate, measured at the side of the cathode for substrates perpendicular to the cathode surface (i.e. not facing the magnetron) [9], it is found that they fit with the axial measurements of J_ρ shown in Figure 6. It is therefore likely that the increasing number of particles transported parallel to the target surface is the reason for the increase in radial energy flux observed around $6 \le z \le 10$ cm in Figure 6. On the other hand, it is also important to take into account the axial variation of energy of the charged species (see for example reference [9] regarding the ion energy distribution, and reference [21, p. 64] regarding the electron energy distribution). Since the thermal probe measurements result in a product of incoming particle flux and particle energy it is difficult with this type of measurement to separate the two parts and determine the dominant factor in the measured total energy flux. Still, it can be concluded that the radial component of the energy flux is substantial.

The question of different contributions from electrons and ions can be partly resolved by measuring the effect of the azimuthally drifting electrons on the energy flux. This was done for three different distances from the magnetron surface and is shown in Figure 7. The probe was placed at ρ = 15 cm and rotated around the axis of the manipulator arm in order to detect flux ranging from radial flux at θ = 0º (essentially the same as in Figure 6) to azimuthal flux at θ = ± 45º. From this figure it is seen that there is an asymmetry in the plotted curve, where a greater energy flux is recorded for positive angles compared to negative angles. A crude estimation of the ratio of energy flux for negative and positive angles can be found by integrating the three different curves separately and comparing the different areas. An average value of 30 % higher energy flux for positive angles was found. By working out the field geometry of the E and B fields it was deduced that for + 45º the probe is facing toward the azimuthally rotating electrons, while rotating the probe to – 45º it is directed away from the electrons. This is in line with previous measurements on electron drift velocities, where the total azimuthal electron drift was found to be about 5×10^4 m/s [18]. Adding this component to the thermal speed of the electrons ($k_B T_e \approx 1.5\,\mathrm{eV}$) for the probe at + 45º and deducting the same value at – 45º we end up with a difference of at least 15 %. It should be pointed out that there is also a small ionic contribution, since the ions are drifting in the same direction. On the other hand the ions have a much larger Larmor radius, around 5-10 cm depending on the axial distance, compared to the electrons (less than a mm), making them unmagnetized in this type of plasma discharge. This means that the ions will be transported away from the cathode surface with only a small drift component in the azimuthal direction. Since the observed asymmetry peaks in the pure azimuthal direction (+ 45º), where the electronic contribution is expected to be the strongest, it is here suggested that the electronic contribution exceeds the ionic one. This will be further explored in the next section using an applied bias on the thermal probe.

3.3. Bias measurements

The effects of biasing the thermal probe are shown in Figure 8. The probe was placed at ρ = 0 cm and z = 10 cm facing the magnetron surface. For a negative potential less than -20 V an almost linear increase can be detected as we approach the ion saturation regime. Here, the deposited heat depends only on the kinetic energy of the ions. If instead looking at the heat flux for positive bias voltage, where most ions are repelled, an exponential increase due to electrons is instead measured. This is consistent with the radial energy flux measurements originating from the azimuthally rotating current in the previous section, where the electrons gave a much larger contribution to the energy flux compared to the ions.

By knowing the plasma conditions the experimental results can be verified through calculations of the energy flux. Due to the dynamic behavior of the HiPIMS pulse, such as a continuous change of all the parameters throughout the pulse as well as the fact that there is a 9.9 ms off-time between two pulses, it is necessary to estimate average values and thus introducing errors in the calculations. In this model only energetic contributions due to charge carriers were taken into consideration. It was here assumed that the mean cathode voltage is $V_{cat} = 440$ V and the secondary electron emission coefficient is $\gamma = 0.05$. In a separate experiment by Sigurjonsson [21] using the same setup and under similar discharge conditions, typical values for the different plasma parameters were found, and we assume an electron density of $n_e = 2\times 10^{18}$ m^{-3}, an electron temperature of $k_B T_e = 1.5$ eV and a plasma potential of $V_{pl} = 3$ V. From investigations on the ion composition in a Ti-Ar plasma by Bohlmark *et al.* [8] the mean charge $(\bar{q} = 1.24\ \text{e})$, the mean ion mass $(\bar{m}_i = 45.44\ \text{u})$ and the mean ionization energy $(\bar{E}_i = 13.51\ \text{eV})$ were extracted by integrating the flux intensity curves of the different ions. The same magnetron and deposition system were also used in this experiment.

The general expression for the energy flux from eq. (5) can thereby be written as

$$J_{tot} = J_i + J_e + J_{e,SE} + J_{rec}, \tag{6}$$

where the energy flux by ions, J_i, is described by the Bohm flux, $j_i = n_e \sqrt{\frac{k_B T_e}{\bar{m}_i}} \exp(-0.5)$ so that

$$J_i = j_i \bar{q}_i \left(V_{pl} - V_s\right), \tag{7}$$

where V_s is the substrate potential due to the applied bias. J_e is the electron energy flux and is given by

$$J_e = n_e \sqrt{\frac{k_B T_e}{2\pi m_e}} \exp\left(-\frac{e\left(V_{pl} - V_s\right)}{k_B T_e} \right) 2k_B T_e \, , \qquad (8)$$

assumed that the electrons have a Maxwellian distribution. The contribution of secondary electrons are taken into account by including the following term

$$J_{e,SE} = j_i \gamma e\left(V_s + V_{cat}\right) . \qquad (9)$$

Furthermore, the recombination energy released at the substrate surface is described by the term

$$J_{rec} = j_i \bar{E}_i \, . \qquad (10)$$

Last, a duty factor of 0.01 was also included, since the pulse is on for about 1 % of the time in the HiPIMS experiments. The model reflects the experimentally obtained results quite well (Figure 8). The nearly constant difference between the model and the experimentally measured curve is likely due to heating by neutrals, particularly energy released by condensation at the substrate surface during film growth [16]. It can be seen that by adding approximately 30 mW/cm^2 of energy flux from neutral species would correct for this difference. Furthermore, heat radiation was not included in the model, but is here expected to be small [2]. The measurements can also be influenced by sputtered atoms from the probe at high negative bias values. This has not been taken into account in the model, but might lower the calculated curve at high negative potentials.

4. Conclusions

Thermal probes were successfully used to measure the energy flux at different positions in a HiPIMS discharge. It was found that the substrate heating is severely reduced in the HiPIMS process compared to conventional DCMS at the same average power. The maximum temperature reached at the substrate position was found to be very low for the HiPIMS discharge making it suitable for coating thermally sensitive substrates. Furthermore, the heating due to radial energy flux reached as much as 60 % of the axial energy flux, which is likely a result of the anomalous transport of charged species present in the HiPIMS plasma.

Finally, the electronic and ionic contributions to the energy flux were separated by using an applied bias to the thermal probe. The experimental results were in good agreement with a model based on energy flux calculations due to charge carriers.

Acknowledgements

The authors wish to thank Mr. Sven Bornholdt for his assistance in the experimental work as well as Dr. Matthias Wolter for his support. This work was partly supported by the Swedish Research Council, the Swedish Foundation for Strategic Research and by the Deutsche Forschungsgemeinschaft under SFB TR 24/B4.

Figures

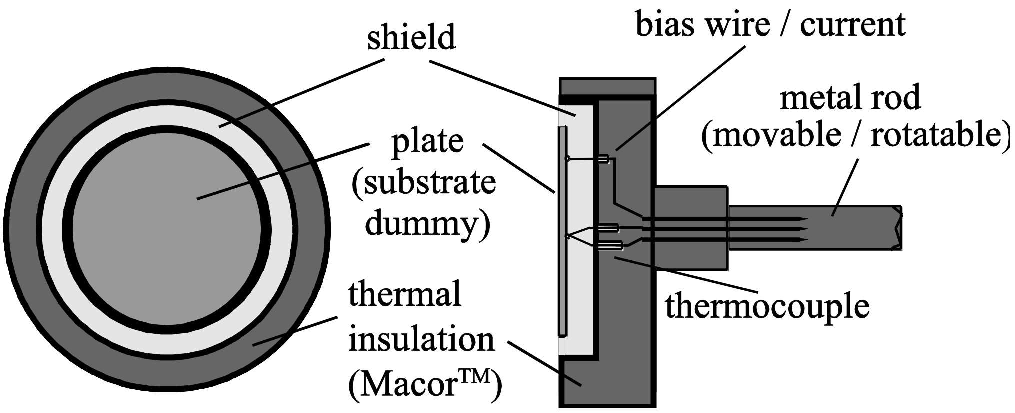

Figure 1. Schematic of the thermal probe used in the experiments.

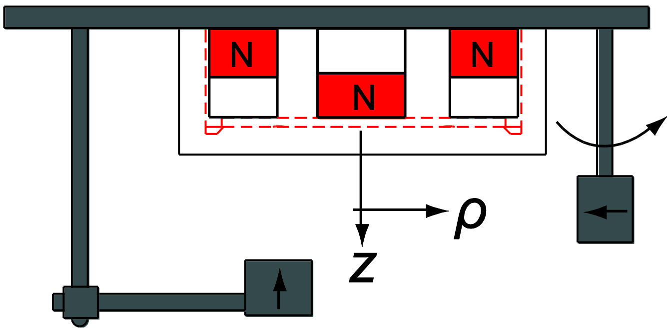

Figure 2. Schematic of the top-mounted magnetron and the probes measuring axial (*z*) as well as radial (*ρ*) energy flux.

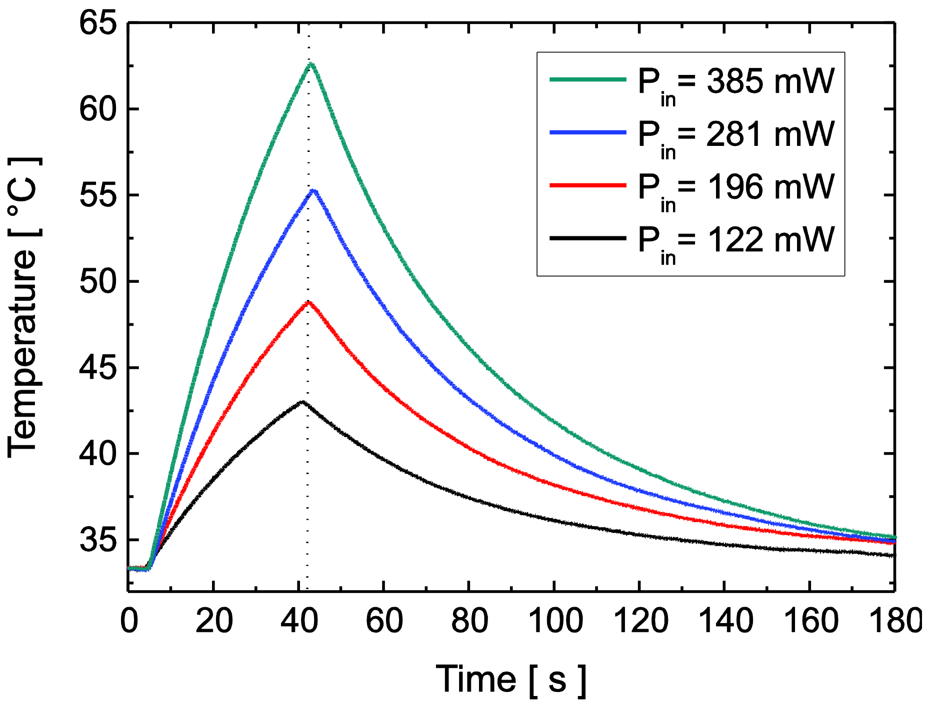

Figure 3. Temperature characteristics from calibration of the thermal probes displaying heating and cooling curves.

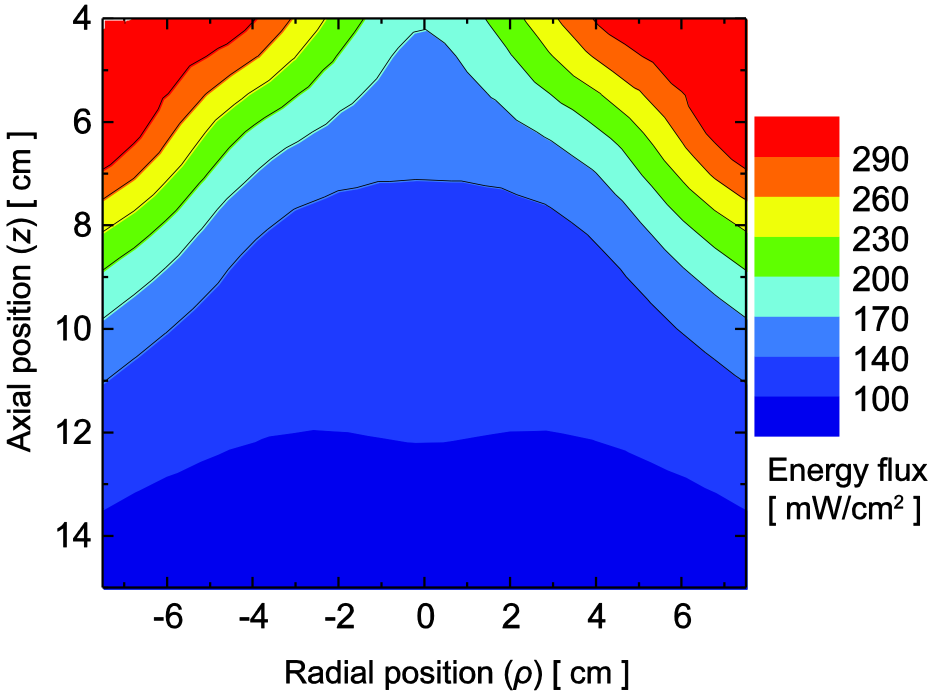

Figure 4. Energy flux using HiPIMS at 500 W measured with the thermal probe facing the magnetron surface.

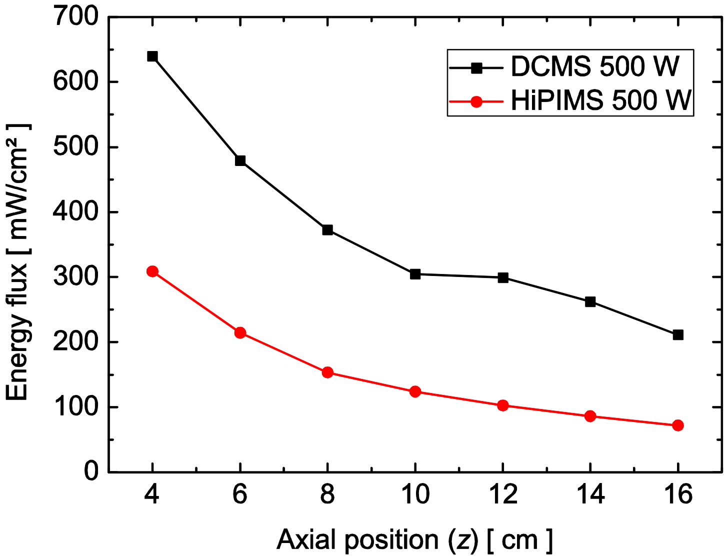

Figure 5. Comparison between HiPIMS and DCMS at approximately the same average power. The probe was placed at ρ = 4.5 cm facing the magnetron surface.

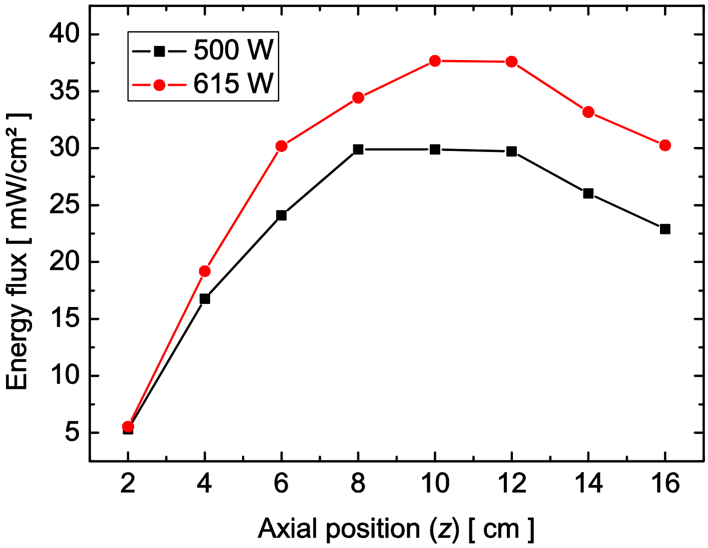

Figure 6. Energy flux measured perpendicular to the magnetron surface when varying the axial position for two different powers. The probe was placed outside the rim of the magnetron at ρ = 15 cm.

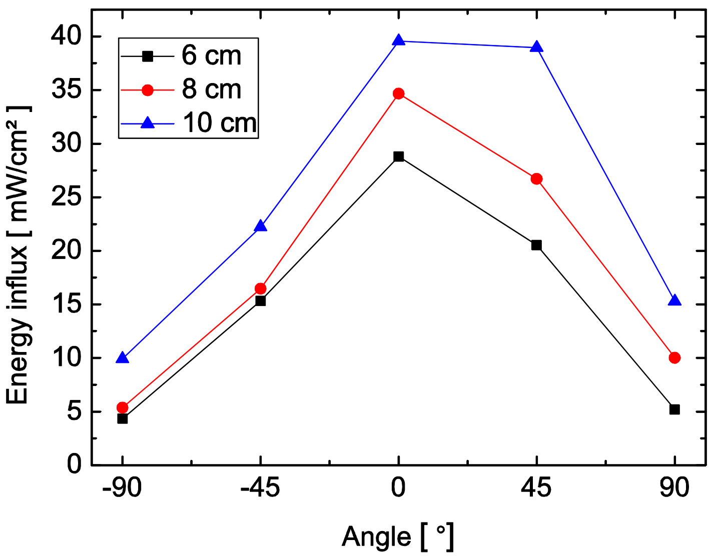

Figure 7. Measuring the energy flux affected by azimuthally drifting electrons for three different distances from the magnetron surface.

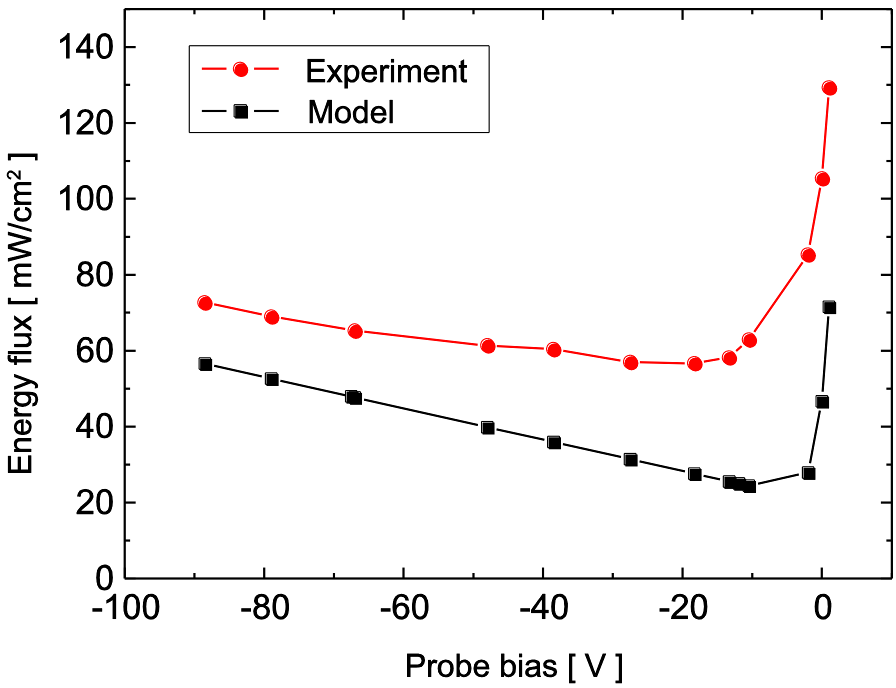

Figure 8. Energy flux measured when biasing the thermal probe. The probe was placed at ρ = 0 cm and z = 10 cm facing the magnetron surface.

References

[1] Thornton J A 1974 *J. Vac. Sci. Technol.* **11** 666

[2] Kersten H, Deutsch H, Steffen H, Kroesen G M W and Hippler R 2001 *Vacuum* **63** 385

[3] Li W, Ma Z Q, Wang Y and Wang D M 2006 *Chin. Phys. Lett.* **23** 178

[4] Petrov I, Adibi F, Greene J E, Hultman L and Sundgren J-E 1993 *Appl. Phys. Lett.* **63** 36

[5] Petrov I, Barna P B, Hultman L and Greene J E 2003 *J. Vac. Sci. Technol. A* **21** S117

[6] Han J G 2009 *J. Phys. D* **42** 043001

[7] Helmersson U, Lattemann M, Bohlmark J, Ehiasarian A P and Gudmundsson J T 2006 *Thin Solid Films* **513** 1

[8] Bohlmark J, Lattemann M, Gudmundsson J T, Ehiasarian A P, Aranda Gonzalvo Y, Brenning N and Helmersson U 2006 *Thin Solid Films* **515** 1522

[9] Lundin D, Larsson P, Wallin E, Lattemann M, Brenning N and Helmersson U 2008 *Plasma Sources Sci. Technol.* **17** 035021

[10] Alami J, Persson P O Å, Music D, Gudmundsson J T, Bohlmark J and Helmersson U 2005 *J. Vac. Sci. Technol. A* **23** 278

[11] Brenning N, Axnäs I, Raadu M A, Lundin D and Helmerson U 2008 *Plasma Sources Sci. Technol.* **17** 045009

[12] Thornton J A 1978 *Thin Solid Films* **54** 23

[13] Wolter M, Stahl M and Kersten H 2009 *Vacuum* **83** 768

[14] Ohring M 2002 *Materials Science of Thin Films* (San Diego, CA, USA) Academic Press p 748

[15] Data sheet: http://www2.dupont.com/Kapton/en_US/assets/downloads/pdf/E_H-78305.pdf accessed 20 March 2009

[16] Kersten H, Rohde D, Berndt J, Deutsch H and Hippler R 2000 *Thin Solid Films* **377-378** 585

[17] Bohlmark J, Helmersson U, VanZeeland M, Axnäs I, Alami J and Brenning N 2004 *Plasma Sources Sci. Technol.* **13** 654

[18] Lundin D, Helmersson U, Kirkpatrick S, Rohde S and Brenning N 2008 *Plasma Sources Sci. Technol.* **17** 025007

[19] Rossnagel S M and Kaufman H R 1987 *J. Vac. Sci. Technol. A* **5** 2276

[20] Bradley J W, Thompson S and Aranda Gonzalvo Y 2001 *Plasma Sources Sci. Technol.* **10** 490

[21] Sigurjonsson P 2008 *Spatial and temporal variation of the plasma parameters in a high power impulse magnetron sputtering (HiPIMS) discharge* (Reykjavik) Faculty of Engineering, University of Iceland